International Journal of Progressive Sciences and Technologies (IJPSAT)
ISSN: 2509-0119.

http://ijpsat.ijsht-journals.org
Vol. 30 No. 1 December 2021, pp.31-57

Performance Of Compressive Sensing Radar Mimo Using Non Uniform Sampling And Orthogonal Matching Poursuit

RANDRIANANDRASANA Marie Emile[1], RAKOTONDRAMANANA Radiarisainana Sitraka[2], RANDRIAMITANTSOA Paul Auguste[3], RANDRIAMITANTSOA Andry Auguste[4]

[1,2]Dept. of Telecommunication, Antsirabe Vankinankaratra High Education Institute,
University of Antananarivo, Madagascar,

[3,4]Dept. of Telecommunication, High School Polytechnic of Antananarivo,
University of Antananarivo, Madagascar,

Abstract—Some of waves are poorly captured by Radar system because of the ionospheric cutoff due to a low frequency. So it becomes difficult to acquire the return signals. A recent paradigm for signal acquisition and reconstruction, known as compressive Sensing (Compressive Sensing, CS), provides a promising data acquisition technique for applications this require a limited number of measurements and leads to the development of a new type of converter : the Analog to Information Converter (AIC). Unlike standard Analog to Digital converters (ADC), AIC can sample at a lower rate than that prescribed by Nyquist Shannon, exploiting the sparsity of signals. The main goal of this article is to study the application of compressed sampling for the acquisition of Radar signals. Based on the characteristic properties of our signals of interest, we progressively and methodologically constructed our acquisition scheme : From the study of signals compressibility, to the choice of the AIC architecture and the signal reconstruction algorithm etc.

Keywords—Compressive Sensing, CS, Radar signals, AIC, Nyquist Shannon.

I. Introduction

The Nyquist Shannon sampling theorem has generally been used as the basis of signal acquisition systems. This theorem places a huge load to process the entire signal, while only a small number of transform coefficients are needed to represent the signal. And the technique to solve this problem is named Compressive Sensing. In the Radar communication system, the application of CS-based reconstruction algorithms reduces the amount of data acquired and provides better signal reconstruction accuracy than existing ones.

II. Radar signal processing

A. Radar equation

The radar equation relates the range of a radar to the characteristic of the transmitter and receiver and the target in the environment. It is useful not only as goal of determining the maximum distance between the radar and the target, but it can also be used as a tool to understand how the radar works. [1] .

The radar equation is then a power budget on the round trip path of an emitted wave. The signal reception power is therefore given by the relation:

$$P_r = \frac{P_t G_t \, G_r \lambda^2 \sigma}{(4\pi)^3 \, (R_t)^2 \, (R_r)^2} \tag{1}$$

Where,

G_t : Transmission antenna gain

G_r : Reception antenna gain

λ : Wavelength

P_r : Power received

P_t : Transmitted power

R_t : Transmitter radar target distance

R_r : Distance between the target and the receiving radar

B. Radar parameter

The radar parameters are as follows [1] :

- Power P_t supplied by the generator (W)
- Antenna gain G
- Frequency f (GHz) or wavelength λ (m)
- Range R_{max}, which is the maximum detection distance;
- Surface Equivalent of Radar SER σ
- Signal to noise ratio $\frac{P_r}{N}$ minimum acceptable at the input of the receiver, value specified by the signal analysis system.
- Receiver bandwidth B (Hz)
- Global noise temperature brought to the input of the receiver $(T_a + T_r)$ in Kelvin.

The first three quantities depend on the transmitter, the last three depend on the receiver.

The range and the effective reflecting surface define the target to be observed, these are the quantities geometric patterns that specify the system. For the radar to work, these eight quantities must be satisfy the equation:

$$\left(\frac{P_r}{N}\bigg|min\right) \leq \frac{\sigma \, G^2 \, P_t}{f^2 \, R_{max}^4 (T_a + T_r) B} \times \frac{c^2}{(4\pi)^3} \tag{2}$$

C. Target distance

In the case of a pulse radar, the distance is calculated from the transit time (go and return) of a short transmitted radio pulse and its propagation speed c. The distance echo (calculated by the radar) is the straight line distance between the radar antenna and the target. The "distance to ground" is the "horizontal" distance between the radar antenna and the target.

$$R = \frac{c \, t}{2} \tag{3}$$

Where : t is the time elapsed between the start and the return of the pulse to the radar.

III. Signal Radar

The radar equation (1) does not specify the nature of the transmitted signal which can be continuous wave, amplitude or frequency modulated, or pulse. Pulse radar is the best known type.

Two general categories of the pulse radar signal are the most common, the constant frequency pulse and the modulated pulse (pulse compression).

D. Constant frequency pulse

The constant frequency pulse is the most classic signal. In addition to its use in conventional radars, it is employed in alternation with the decompressed pulse in pulse compression radars to cover the near blind area.

This pulse is characterized by its constant frequency, its rectangular shape and its short duration which defines the resolving power of the radar. The expression of the impulse can be written as follows:

$$r(t) = u(t)e^{(2\pi f_c t+\phi)} \tag{4}$$

Where $u(t)$: the complex envelope of the transmitted signal expressed by :

$$u(t) = \begin{cases} A\ si\ 0 \leq t \leq T \\ 0\ ailleurs \end{cases} \tag{5}$$

f_c : transmission frequency (carrier)

ϕ : initial phase

For electronic warfare countermeasures and performance reasons, radars often use phase coding from one pulse to another (change of ϕ from one pulse to another according to a well-determined code).

E. Pulse compression

Pulse compression is a signal processing technique used in radar, sonar, seismic, and other systems. In the radar context, pulse compression is designed to minimize the peak transmitted power, maximize the signal-to-noise ratio, and have good resolution. Two intra-pulse modulations are most commonly used, frequency modulation and phase modulation.

- Modulation de fréquence

The simplest approach to this type of frequency modulation is Linear Frequency Modulation (LFM). The carrier frequency varies linearly, within a range Δf, during the T-pulse, which broadens the spectrum of the transmitted signal. The major constraint of pulse compression is the appearance of sidelobes in the compressed signal that can degrade radar resolution. Techniques to reduce sidelobes are used in radar, such as weighting or filtering.

- Phase encoding

One of the first methods of pulse compression is phase encoding [1][3]. The pulse of duration T, is divided into L intervals of identical duration, and each interval is assigned a phase value.

The complex envelope of the phase-coded pulse is given by :

$$r(t) = \frac{1}{\sqrt{T}} \sum_{l=1}^{L} r_l\, rect\left[\frac{t-(l-1)t_p}{t_p}\right] \tag{6}$$

Where : $r_l = e^{j\psi_l}$ and the L phase system $\psi_1, \ldots, \psi_L$ is the phase code associated with $r(t)$; $t_p = T/L$

The search for a sequence of L phases (or codes) for different radar applications has occupied radarists for a very long time.

There are an unlimited number of possibilities to generate a sequence of phases of length L.

IV. RADAR MIMO

F. MIMO radar processing chain

The entire MIMO radar processing chain is described in Figure 1.

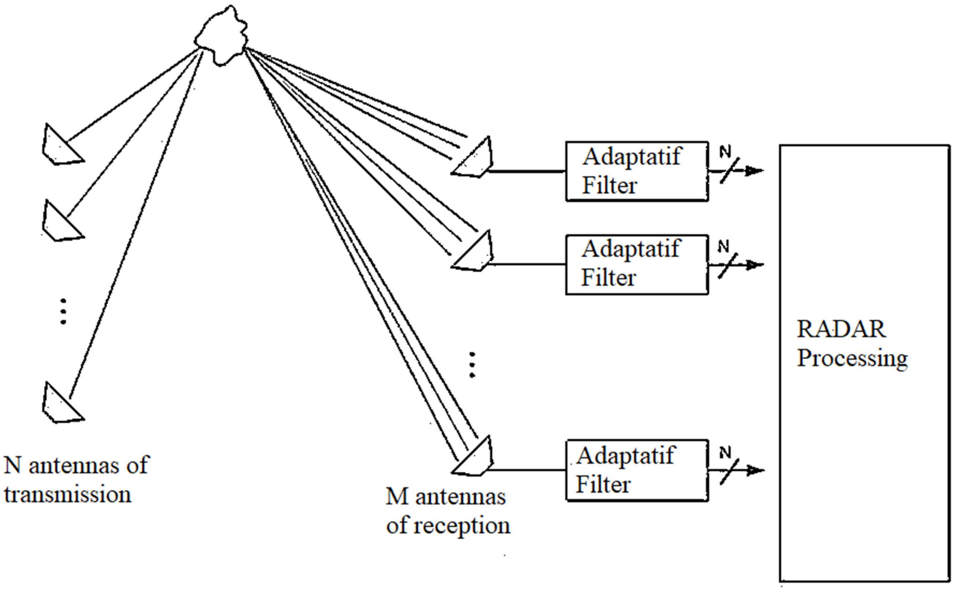

Fig. 1. MIMO radar processing chain

Each receiving antenna therefore receives all signals from the transmitting antennas. First, each antenna is processed using appropriate filters to separate the different signals received (MIMO separation). Then, when all the received signals are separated, specific radar processing techniques are applied to produce the radar image [2].

G. Phased array radar

The phased array radar uses antenna arrays to transmit and receive signals. These arrays can be linear or planar :

In linear or surface networks, the separation between elements is generally uniform. These networks can be co-located and even transmit and receive functions can be performed by the same network.

The two arrays can also be widely separated allowing the radar system to operate in bistatic mode. When the spacing between the array elements is small, the bistatic SER seen by each transmit-receive pair in such a system is assumed to be the same. In phase-shifted array radars, each antenna element in the transmission array sends an dephased offset version of the same waveform. [3]

Consider a phased array radar system that has n_T transmission elements and n_R reception elements. Assume that the transmitting and receiving networks are uniform linear networks with element spacing d_T and d_R respectively.

The received signal pattern is expressed as :

$$y(t) = \sqrt{\frac{E_T}{n_T}} n_R n_T \gamma' + \eta(t) \tag{7}$$

Where : E_T is the average total transmitted energy and γ' represents the backscatter effect

$\eta(t)$ is a zero-mean vector of complex random processes that is of the form :

$$\eta(t) = \begin{pmatrix} \eta_1(t) \\ \eta_2(t) \\ \vdots \\ . \\ \eta_{n_R}(t) \end{pmatrix} \tag{8}$$

If the received signal is sent to a suitable filter to $x(t) = a(\breve{\theta})\sqrt{\frac{E_T}{n_T}}x(t)$, where $a(\breve{\theta})$ is the director vector of the transmitter. And the output is sampled at time δ.

The output of the matched filter becomes :

$$y(t) = \sqrt{\frac{E_T}{n_T}} b^H(\breve{\theta}')b(\theta')a^H(\theta)a(\breve{\theta}')\gamma' + \eta(t) \tag{9}$$

Where $a(\breve{\theta}')$ is expressed by:

$$a(\breve{\theta}') = \begin{pmatrix} 1 \\ e^{\frac{j2\pi d_T sin(\breve{\theta}')}{c}} \\ \vdots \\ \vdots \\ e^{\frac{j2\pi f(n_T-1)d_T sin(\overline{\theta}')}{c}} \end{pmatrix} \tag{10}$$

and $b(\theta')$ is :

$$b(\theta') = \begin{pmatrix} 1 \\ e^{\frac{-j2\pi d_T sin(\breve{\theta}')}{c}} \\ \vdots \\ \vdots \\ e^{\frac{-j2\pi f(n_T-1)d_T sin(\breve{\theta}')}{c}} \end{pmatrix} \tag{11}$$

For the case of phased array radar, a channel matrix can be defined as::

$$H = b(\theta')a^H(\theta)\gamma' \tag{12}$$

H. Coherent MIMO radar

The coherent MIMO radar system uses antenna arrays to transmit and receive signals.

These networks can be co-located and even the transmission and reception functions can be performed by the same network; or the networks can be separated.

Regardless of the separation between the array elements is, the key in coherent MIMO radar is that the array elements are close enough that each element sees the same aspect of the target, i.e. the same SER. Coherent MIMO radar resembles phased array radar because of this deployment pattern of the antenna elements. However, each antenna in the coherent MIMO radar sends out different waveforms.

Consider a coherent MIMO radar system that has n_T transmit elements and n_R receiving elements.

The received signal model is given by :

$$y(t) = \sqrt{\frac{E_T}{n_T}} Hx(t-\delta) + n(t) \tag{13}$$

Where E_T is the average total transmitted energy and γ' represents the backscatter effect.

$\eta(t)$ is a zero mean vector of complex random processes.

If this received signal is sent to an array of matched filters, each of which is matched to $x_m(t)$, and the corresponding output is sampled at time instants δ.

The output of the series of matched filters can be written as a vector :

$$\bar{y}(t) = \sqrt{\frac{E_T}{n_T}} \bar{\gamma}' + \bar{\eta}(t) \tag{14}$$

Where $\bar{y}$ is a complex vector $n_T n_R \times 1$ whose inputs correspond to the outputs of each adaptive filter of each receiver, $\bar{\eta}$ is a complex noise vector $n_T n_R \times 1$, and $\bar{\gamma'}$ a complex vector defined by :

$$\bar{\gamma'} = [b^*(\theta') \otimes a^*(\theta')\,] \tag{15}$$

Where $\otimes$ denotes the Krönecker product..

Note that the distribution of each $\bar{\gamma'}$ is equal to the distribution of γ' when the elements of $b^*(\theta')$ and $a^*(\theta')$ are on the unit circle, such that :

$$b^*(\theta') = \begin{pmatrix} e^{-j2\pi f \breve{\delta}_{T_1}(\theta\prime)} \\ e^{-j2\pi f \breve{\delta}_{T_2}(\theta\prime)} \\ \cdot \\ \cdot \\ e^{-j2\pi f \breve{\delta}_{T_{n_T}}(\theta\prime)} \end{pmatrix} \tag{16}$$

$$a^*(\theta') = \begin{pmatrix} e^{-j2\pi f \delta_{T_1}(\theta\prime)} \\ e^{-j2\pi f \delta_{T_2}(\theta\prime)} \\ \cdot \\ \cdot \\ e^{-j2\pi f \delta_{T_{n_T}}(\theta\prime)} \end{pmatrix} \tag{17}$$

For the case of coherent MIMO radar, a channel matrix can be defined as :

$$H = \gamma' b^*(\theta') a^H(\theta) \tag{18}$$

I. Statistical MIMO Radar

The spacing between elements in an array is also so large that each transmit-receive pair sees a different aspect of the target and thus sees different SERs due to the complex shape of the target. If the spacing between the antenna elements is large enough, the signals received from each transceiver pair become independent. This is called spatial diversity or angular diversity. Statistical MIMO radar focuses on this property. [2] [3]

Consider a statistical MIMO radar system that has n_T elements and n_R reception elements.

The received signal is given by :

$$y(t) = \sqrt{\frac{E_T}{n_T}} Hx(t-\delta) + n(t) \tag{19}$$

Where E_T is the average total transmitted energy and γ' represents the backscatter effect

$\eta(t)$ is a zero mean vector of complex random processes.

If this received signal is sent to a row of adaptative filters each of which is adaptative to $x_m(t)$, and the corresponding output is sampled at the instants of time δ.

The output of the series of matched filters can be written as a vector :

$$\bar{y}(t) = \sqrt{\frac{E_T}{n_T}} \overline{\gamma'} + \bar{\eta}(t) \tag{20}$$

Where $\overline{y}$ is a complex vector $n_T n_R \times 1$ whose inputs correspond to the outputs of each adaptive filter of each receiver, $\overline{\eta}$ is a complex noise vector $n_T n_R \times 1$, and $\overline{\gamma'}$ vector complex

The equation (20) can be rewritten in an explicit form such as :

$$\begin{pmatrix} y_{11} \\ y_{12} \\ \cdot \\ \cdot \\ y_{n_R n_T} \end{pmatrix} = \sqrt{\frac{E_T}{n_T}} \begin{pmatrix} \gamma_{11} \\ \gamma_{12} \\ \cdot \\ \cdot \\ \gamma_{n_R n_T} \end{pmatrix} + \begin{pmatrix} \eta_{11} \\ \eta_{12} \\ \cdot \\ \cdot \\ \eta_{n_R n_T} \end{pmatrix} \tag{21}$$

For the static MIMO radar case, a channel matrix can be defined as :

$$H = diag\left(b(\theta')\gamma' diag\big(a(\theta)\big)\right) \tag{22}$$

V. THEORY OF COMPRESSIVE SENSING

J. Nyquist-Shannon

In the field of digital signal processing (Figure 6), it is customary to refer to the Nyquist-Shannon theorem to faithfully reconstruct a signal of width spectral and amplitude-limited: This theorem, also known as the sampling theorem, states that the exact reconstruction of a band-limited signal requires that the frequency of sampling is greater than or equal to twice the width of its spectrum (i.e. the difference between the minimum and maximum frequencies it contains) [4].

Except that usually, after this sampling phase, and due to transmission or storage restrictions, a compression step is performed.

One of the most popular compression techniques is sparse decomposition compression : signals can be sparse or compressible in the sense that they have concise representations in bases or well-chosen dictionaries.

Thus, we can cancel a large part of the small coefficients without perceptible loss.

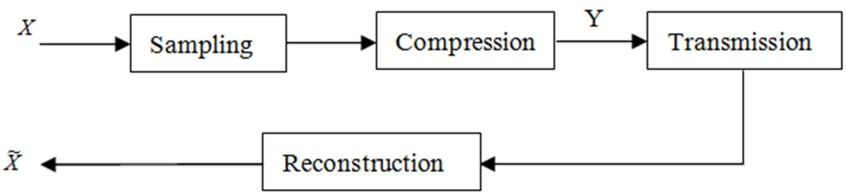

Fig. 2. Conventional approach to digital signal processing

This strategy is adopted by most modern compression standards, especially in the area of image processing, such as JPEG-2000. First a sparsifying transform is applied to the image, translating the input signal into a vector of coefficients, then this sparsifying vector is encoded by selecting the most significant coefficients and ignoring the smaller ones. The compressed data Y will then be transmitted and finally reconstructed. This approach works well in many applications.

However, acquiring many samples and then ignoring many of them is extremely expensive. The main idea of compressed sampling is, as its name suggests, to directly capture the data in a compressed form by exploiting the sparse of the signal (Figure 7): instead of generating N samples, the goal is to generating only M measurements (M << N) such that their acquisition allows efficient reconstruction of the input signal. Thus, compressed acquisition makes it possible to capture a signal at a frequency significantly lower than the Nyquist frequency.

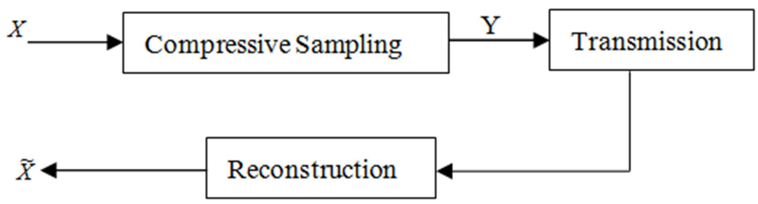

Fig. 3. Compressive sensing paradigm

K. Signal acquisition

Mathematically, CS is defined by [5]:

$$Y = \Phi X + Z \tag{23}$$

Y represents the compressed data that will be digitized by the ADC or Analog digital Converter quantizer, it is formed by M measurements. X is the unknown signal formed by N samples. Φ is the matrix of measurement matrix (Gaussian, Bernoulli, Discret Fourier Transform or DFT etc.) of size M x N, with N > M, modeling a subsampling and Z is an unknown noise term (quantization noise, thermal noise, etc.)

L. Signal reconstruction

Reconstruction takes more time and power than acquisition. For most CS applications, this step is not implemented on the circuit with the step of the acquisition. [6]

According to equation (23), to reconstruct the signal X from the recovered measurements,

there are more unknowns than equations (N> M). We have in the case of an under-determined system. Mathematically, this system has an infinity of solutions. In order to solve this problem, the CS is essentially based on two notions: the sparse (or the compressibility) of the signal, and the verification of the restricted isometric property (RIP) by the measurement matrix (or the inconsistency between the measurement matrix and the basis of sparse).

M. Sparse and compressibility

All intelligence resides in a priori knowledge of the signal. In the case of CS, we are interested in sparse or compressible signals. Thre sparse expresses the idea that the information rate of the signal is smaller than that suggested by its bandwidth.

In CS, the more signal sparse, the lower the number of samples required for its reconstruction.[4][7]

A signal is K parsimonious in a database or dictionary if it can be described by a small number K of non-zero coefficients in this base / dictionary (K << M <N). He is expressed by:

$$X = \psi S \tag{24}$$

With S the sparse representation of X such that $||S||_0 \leq K$ and Ψ is the basis of parsimony of dimension N x N.

Equation (25) becomes :

$$Y = \Phi\psi S + Z \tag{25}$$

Few natural signals are sparse : when we talk about sparse in CS, we are actually talking about compressibility. Intuitively, this means that the signals can be represented by a few significant coefficients while the others are close to zero. Figure 4 illustrates the difference between these two concepts.

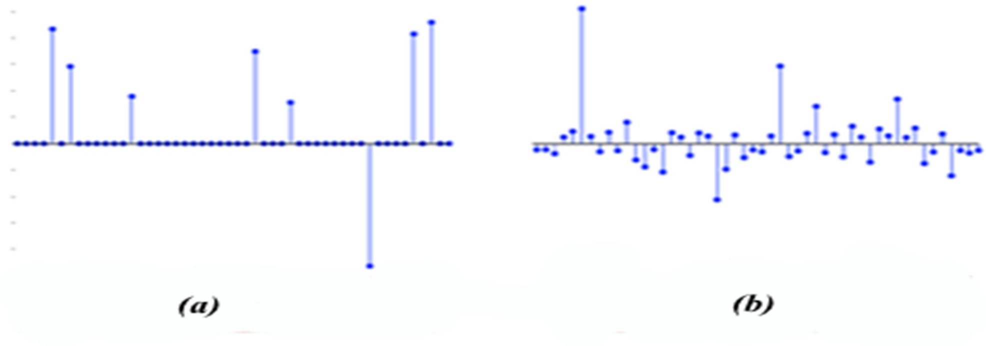

Fig. 4. Sparse signal (a) and compressible signal (b)

Mathematically, a signal is compressible if the module of its coefficients sorted in Ψ follow a decrease in power law:

$$|S_i| \leq Ci^{-q}\,; i = 1,2, \dots N \tag{26}$$

Where ***C*** is a constant. The larger q is the degradatation of the signal and the more compressible the signal will be.

N. RIP and inconsistency

The CS chooses a K-sparse solution among the possible solutions of the equation (23). The existence of the solution is trivial. On the other hand, its uniqueness and its stability are not guarantees. One of the major contributions of the first work on CS is the definition of the mathematical framework to satisfy the uniqueness and the stability of the K-sparse solution. For this, other conditions must be considered on the acquisition method.

In particular a condition which ensures a good reconstruction of the data, is to check that the matrix $A = \Phi\Psi$ satisfies the restricted isometric property (RIP).[8]

Matrix A satisfies the RIP of order K if there is an isometric constant $\delta_K \in]0,1[$ such that for any K-sparse vector, we have the following frame:

$$(1 - \delta_K) \leq \frac{\|AS\|_2^2}{\|S\|_2^2} \leq (1 + \delta_K) \tag{27}$$

δ_K is the smallest number which ensures this framing for any K-sparse vector.

Intuitively, the order RIP *k* means that the measurement matrix approximately preserves the norm of any K-sparse vector. The random matrices satisfy the RIP with a very high probability with certain conditions on the number of measurements. For example, it was demonstrated that random matrices with Gaussian or sub-Gaussian inputs satisfy the RIP with a high probability provided tha t$M = 0\ (KlogN)$.

The RIP condition is a sufficient condition to allow the resolution of the equation of CS. It ensures the uniqueness of the solution and its stability for $\delta_K < \sqrt{2} - 1$. Unfortunately, RIP is a difficult NP problem. It is difficult to construct matrices satisfying this property with certainty and to verify it. There is another theoretical approach to compressed acquisition based on the notion of the inconsistency between the measurement matrix and the sparse basis.

Consistency between *Φ* and *Ψ* is expressed by :

$$\mu(\phi, \psi) = \sqrt{(N)}\, \underset{1 \leq u, j \leq N}{max} |< \Phi_u, \psi_j >| \tag{28}$$

With $1 < \mu(\phi, \psi) < \sqrt{(N)}$ is the set of consistency values between a line of *Φ* and a column of *Ψ*. The lower the consistency, the lower the number of measurements required for reconstruction and the greater the compression factor. [9]

Intuitively, low coherence means that the signal which is sparsed in Ψ has a dense representation in Φ. An example of two inconsistent bases is the time frequency duality : a Dirac or a peak in the time domain is spread out in the frequency domain. Conversely, a frequency is spread into a pure sine wave in the time domain.

Compressed sampling theory based on this approach states that if we perform M measurements using linear random projections, i.e. by taking the product of the input signal with a random measurement matrix, then the number of measurements needed to recover X with a high probability is:

$$M \geq Cu^2(\phi, \psi)\; K \log(N) \tag{29}$$

In the case where the measurement matrix is completely inconsistent with the sparse basis, the minimum number of random measurements to have a high probability, a good reconstruction is:

$$M \geq \log(N) \tag{30}$$

Note that some random matrices are largely inconsistent with any fixed bases. Indeed, if we choose an orthonormal measurement matrix whose columns are taken in a uniformly random manner then, with a very high probability, the consistency between the measurement matrix and the parsimony basis is of the order of $\sqrt{2logN}$. This is why a Bernoulli matrix, composed of random ± 1 binary inputs, or a Gaussian matrix are highly inconsistent with any basis of sparse.

VI. GREEDY RECONSTRUCTION ALGORITHMS

Several reconstruction techniques have been explored to recover the sparse solution from a reduced number of measurements. Greedy algorithms are signal processing techniques, called sparse decomposition techniques. The idea is to iteratively construct a sparse approximation of the signal. [10]

Greedy algorithms build from an initial value $X_0 = 0$, at each iteration, an approximation X_k signal and evaluates a residual error. The operation is repeated until a stop criterion set by the user. .

O. Matching Pursuit

We have a measurement vector Y and a matrix A = ΦΨ and we want to write Y as a linear combination of elements a_i of A or at least approach Y by such a linear combination, in other words reconstruct the signal X. The MP proposes a simple approach: At the start, the residue r is initialized with the measurement vector Y and the approximation of the signal $\widehat{X}$ by a zero vector such that $r_0 \leftarrow Y$ and $\widehat{X} \leftarrow 0$.

At each iteration k, the algorithm will have to choose the column a_i of the matrix A most correlated to the measurement vector Y. The standard MP algorithm uses the dot product as the correlation function.

$$\lambda_k = argmax|< r_{k-1}, a_i >| \tag{31}$$

Where,

λ_k is the index of the selected column;

r_{k-1} is the residual of the previous iteration;

a_i represents the column of matrix A with $1 \leq i \leq N$, they are also called atoms.

Then, the MP constructs a new approximation of the signal by adding to $\widehat{X_k}$ the projection of the residue on a_k , then it updates the residual signal (this is called the residue) $r_k = Y - Y_k$

$$\widehat{X_k} = \widehat{X_{k-1}} + < r_{k-1}, a_k >. a_k \tag{32}$$

$$\widehat{X_k} = \widehat{X_{k-1}} + < r_{k-1}, a_k >. a_k \tag{33}$$

Where,

$\widehat{X_{k-1}}$ represents the approximation of the signal obtained during the previous iteration;

r_k is the column of the selected matrix A.

The process is repeated until the signal is broken down satisfactorily, that is, until the stop condition is met. The criterion for stopping this algorithm may be :

- A residual error below a given threshold
- A maximum number of iterations;
- A criterion of calculation time, memory, etc.

The description of the MP algorithm is as follows:

Algorithm 1 : $x = MP(y, \phi)$

$\boldsymbol{initialization : k = 1,}$
$\boldsymbol{\varepsilon^0 = y, dictionnary\ D^0} = \emptyset$
$\boldsymbol{repeat}$
$\quad \boldsymbol{for}\ m \leftarrow 1, M\ do$
$\qquad Scalar\ products :\ C_m^k \leftarrow \langle e^{k-1}, \phi_m \rangle$
$\quad \boldsymbol{end\ for}$
$\quad Selection :\ m^k \leftarrow \arg max_m \lvert C_m^k \rvert$
$\quad Actif\ dictionnary : D^k \leftarrow [D^{k-1}, \phi_{m^k}]$
$\quad Actif\ coeffcient: x^k \leftarrow [x^{k-1};\ C_{m^k}^k]$
$\quad Residue :\ e^k \leftarrow e^{k-1} - C_m^k \phi_{m^k}$
$\qquad k \leftarrow k + 1$
$\boldsymbol{until}\ (satisfied\ stopping\ criteria)$

P. **Orthogonal Matching Pursuit**

In the OMP we also select the atoms a_i one by one but with each new atom selection, we choose as a new approximation the orthogonal projection of the starting signal Y on the subspace generated by all of these atoms $(a_j \text{ for } j = 1 \dots k)$. This update rule makes that after k iterations, $\forall\ i = 1 \dots k, < a_i, r_k\ >= 0$,

so that with each iteration a new atom will be selected. Thus, the OMP performs a maximum of M iterations for a measurement vector Y having M elements.

The description of the OMP algorithm is as follows:

Algorithm 2 : $x = OMP(y, \phi)$

$\boldsymbol{initialization} : \boldsymbol{k = 1},$

$\boldsymbol{\varepsilon^0 = y, dictionnary\ D^0} = \emptyset$

$\boldsymbol{repeat}$

$\quad \boldsymbol{for}\ m \leftarrow 1, M\ faire$

$\qquad Scalar\ products:\ C_m^k \leftarrow \langle e^{k-1}, \phi_m \rangle$

$\quad \boldsymbol{end\ for}$

$\quad Selection:\ m^k \leftarrow \arg max_m\, |C_m^k|$

$\quad Actif\ dictionnary : D^k \leftarrow \left[D^{k-1}, \phi_{m^k}\right]$

$\quad Actif\ coeffcient :$

$\qquad x^k \leftarrow \arg min_x\, \left\| y - D^k x \right\|_2^2$

$\quad Residue:\ e^k \leftarrow y - D^k x^k$

$\qquad k \leftarrow k + 1$

$\boldsymbol{until}\ (satisfied\ stopping\ criteria)$

.

II. Non-uniform sampling architecture (CS-NUS)

It is an architecture suitable for sparse signals in the frequency domain $\left(\psi = DFT^{-1}\right)$.

It is based on the principle of time-frequency duality: Indeed, the time and frequency domains are inconsistent with each other. So for a sparse signal in the frequency domain and applying the probabilistic approach of compressed acquisition, it suffices to acquire samples in the time domain in a non-uniform and arbitrarily spaced way. [11] [12] [13]

The idea behind the NUS is schematized in Figure 5. For the sake of didacticism, suppose that there is an ADC which samples the input signal at the Nyquist frequency. A Pseudo-Random Bit Sequence (PRBS) controls which of these samples are collected and which are ignored. Of all the N samples at the Nyquist frequency, only M≪N are collected.

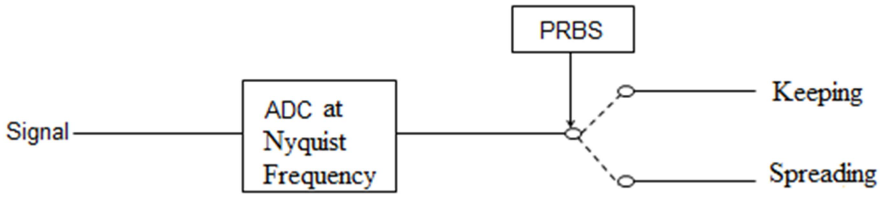

Fig. 5. Conceptual diagram of the NUS architecture

The aim of the CS is to obtain an average sampling frequency lower than the Nyquist frequency. Also, in practice, non-uniform sampling based on the principle of compressed sampling (CS-NUS) chooses samples arbitrarily spaced by an integer number of clock periods at the Nyquist frequency.

The measurement matrix corresponding to this architecture is a rectangular matrix of $M \times N$ presented by ΦNUS : in each row of the measurement matrix, there is only one coefficient not zero and equal to 1. The location of this coefficient in the line is random, this allows to define a sample among N which will be taken in a random way. An example of measurement matrix ϕ_{NUS} is illustrated by :

$$\phi_{NUS} = \begin{pmatrix} 1 & 0 & 0 & 0 & 0 & \dots & 0 \\ 0 & 0 & 1 & 0 & 0 & \dots & 0 \\ & & & \ddots & & & \\ 0 & 0 & 0 & 0 & \dots & 1 & 0 \end{pmatrix}_{M \times N} \quad (34)$$

VII. Compressive Sensing Parameters

A. Measurement matrices and consistency between the matrix $\psi_{DFT^{-1}}$ and measurement matrices

Figure 6 reports the consistency between the matrix $\psi_{DFT^{-1}}$ and some measurement matrices

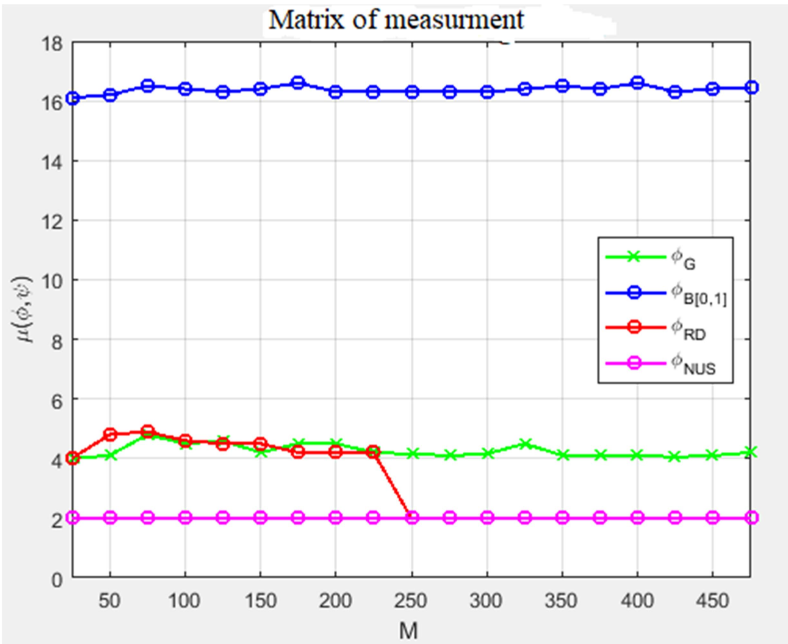

Fig. 6. *Coherence μ between $\psi_{DFT^{-1}}$ and matrix of measurement ϕ*

- ϕ_G : Matrix whose elements are generated from a Gaussian random process with zero mean and variance $1/M$
- $\phi_{B[0,1]}$: Matrix whose elements are generated from a Bernoullian random process and take values in {0, 1}.
- ϕ_{RD} : Random demodulator measurement matrix
- ϕ_{NUS} : Non-uniform sampler measurement matrix

These results were obtained for N = 500 and M variant of 25 to 475. The coherences between the matrix $\psi_{DFT^{-1}}$ and the Gaussian and Bernoullian random matrices remain almost constant independently of the value of M. They vary around 4.5. Consistencies between the base sparse matrix $\psi_{DFT^{-1}}$ and matrix ϕ_{RD} tends to 2 when the value of M increases. Recall that the lower bound of consistency is 1. The three curves converge from M = 100.

These results show that eliminating: the random permutation of the columns and the generation of the random values of the blocks forming the diagonal does not affect the consistency between the measurement matrix and $\psi_{DFT^{-1}}$. For the case of ϕ_{NUS} , consistency remains constant, the value of which is 2.

Non-uniform sampling exploits the inconsistency between time and frequency to downsample the signal.

The measurement matrix modeling the under-sampling is the canonical matrix which is inconsistent with the DFT^{-1} .

The location of this coefficient in the row is random, which makes it possible to define a sample among N which will be taken in a random manner. In our study, we will focus on this type of architecture (figure 7). [15]

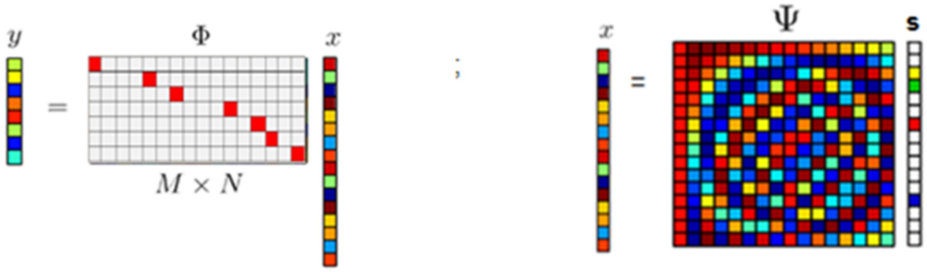

Fig. 7. *Matrix of measurement ϕ for the NUS architecture*

B. Reconstruction algorithm and reconstruction quality evaluation metrics

The quality of the reconstructed signal is evaluated by measuring the distortion between the original signal x and the reconstructed one $\breve{x}$. We use the " Percentage Root-mean-square Deviation (PRD) » and the « Signal to Noise Ratio (SNR) » [15] :

$$PRD[\%] = \frac{\|x - \breve{x}\|_2}{\|x\|_2} \times 100 \tag{35}$$

$$SNR[dB] = 20log_{10}\frac{\|x - \breve{x}\|_2}{\|x\|_2} \tag{36}$$

Where x and $\breve{x}$ representes the original signal and reconstructed signal.

The value of the PRD makes possible to define the quality of the reconstructed signal.

And the compression ratio ("Compression Ratio (CR)") and the Compression Factor ("compression factor (CF)") define as follows :

$$CR[\%] = \frac{N - M}{N} \times 100 \tag{37}$$

$$CF = \frac{N}{M} \tag{38}$$

Where, M and N are respectively the numbers of rows and columns of the measurement matrix ϕ.

As concrete examples, we took sinusoidal signals from the Matlab database. We have divided the signals into blocks of N consecutive samples. We compressed each block with the NUS measurement matrix, then we reconstructed each block respectively with the two reconstruction algorithms. When the signals are fully reconstructed, we evaluated their PRD and SNR.

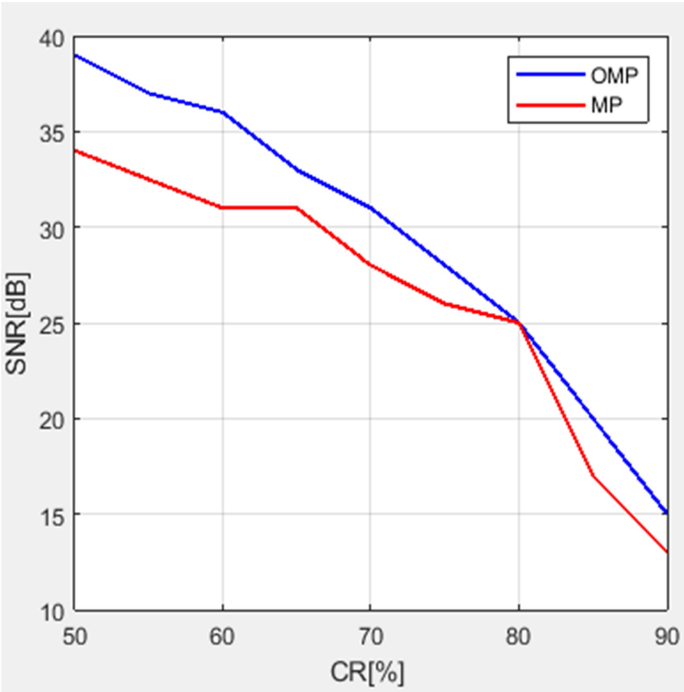

Fig. 8. *SNR as a function of compression ratio for sinusoidal signals*

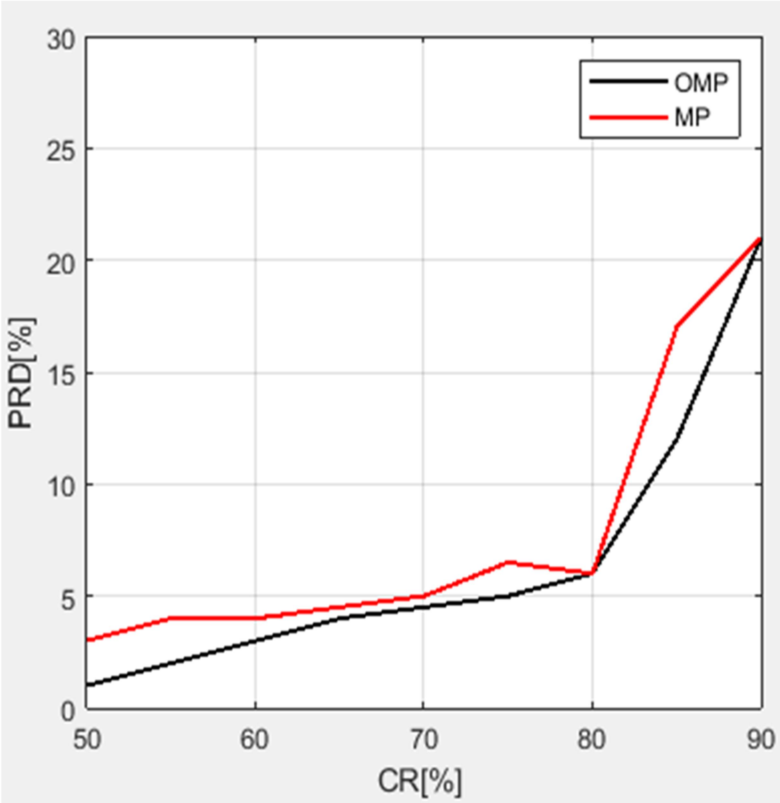

Fig. 9. *PRD as a function of compression ratio for sinusoidal signals*

Figure 8 and Figure 9 report SNR and PRD as a function of compression ratio. The more the compression rate increases, the more the quality of the reconstructed signal is not degraded. We got a higher SNR and a lower PRD. This is because sinusoidal signals are more parsimonious in this area.

C. Norme L_p

In this section we will deal with discrete signals of finite length which are modeled by vectors in a Euclidean space of dimension $N(\mathbb{R}^N: X = X_1, X_2, \dots X_N)$. In this case, the norm of L_p is defined by [16] :

$$\|X\|_p = \left(\sum_{i=1}^{N} |X_i|^p\right)^{1/p} \quad p \in [1, \infty[\tag{39}$$

Standards are primarily used to measure the strength of a signal or the margin of an approximation error. The choice of standard L_p influences the properties of the resulting approximation error. Large "p" values tends to distribute the error more evenly among the signal coefficients, while small values lead to an error that is more unevenly distributed and tends to be more parsimonious.

This intuition generalizes to higher dimensions and explains the focus on the norm L_1 for the reconstruction of parsimonious signals.

D. Radar signal compressibility

We can classify the bases of parsimony in two categories : The usual bases (Fourier, identity, wavelet, etc.) and the bases / dictionaries built from sufficiently long training examples of the studied signal. The compressibility of the signal can be studied in different domains: such as the compressibility of the signal in the time domain $(\psi = Identité)$, in the frequency domain

$\left(\psi = DFT^{-1}\right)$ and in the time-frequency domain with different wavelet families that have a waveform close to the signal waveform [15].

Recall that a signal is compressible in a domain if the moduli of these coefficients $(|S_i|)$ sorted in ψ decrease rapidly. In addition, the faster the decay, the more compressible the signal will be.

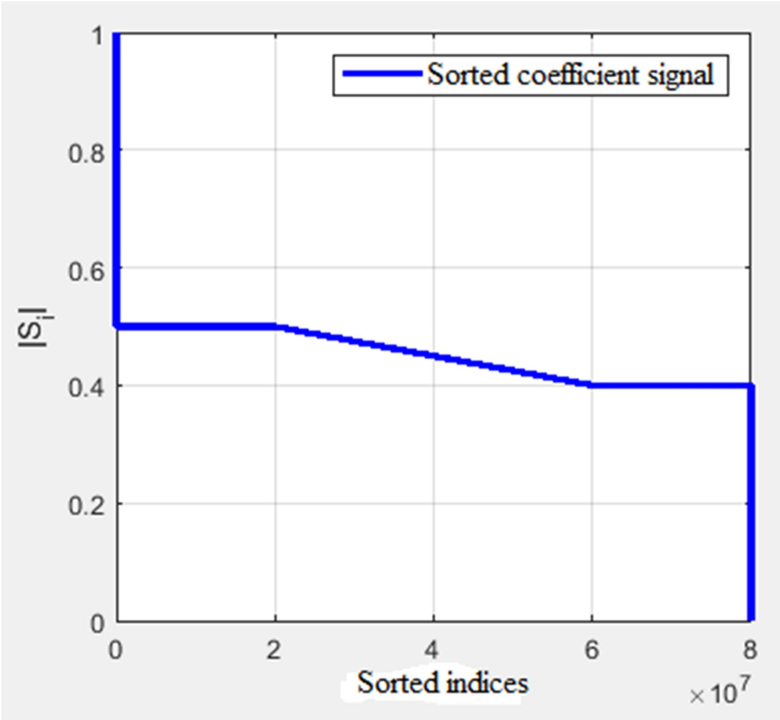

Fig. 10. *Time domain radar signal compressibility*

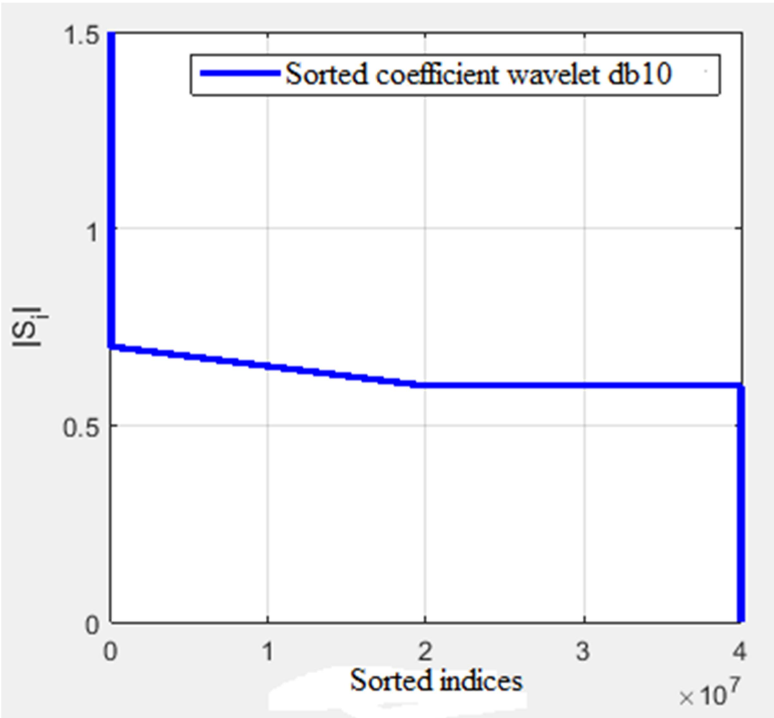

Fig. 11. *Compressibility of the Radar signal in frequency time with a dB10 wavelet*

Figures 10, 11, 12 and 13 illustrate respectively the compressibility of the Radar signal in the time domain, in the time frequency domain with a Daubechies10 wavelet and in the frequency domain.

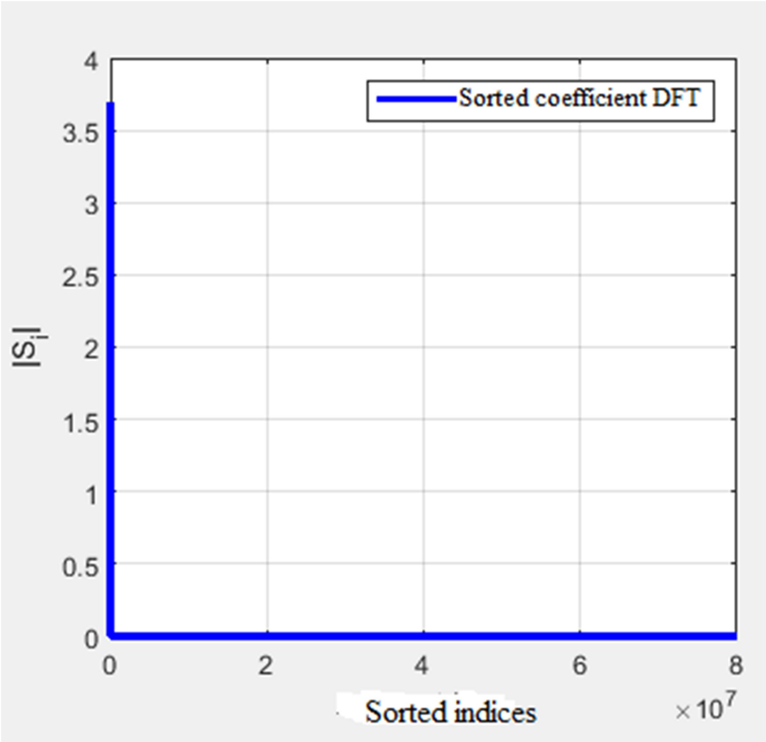

Fig. 12. *Compressibility of the Radar signal in the frequency domain*

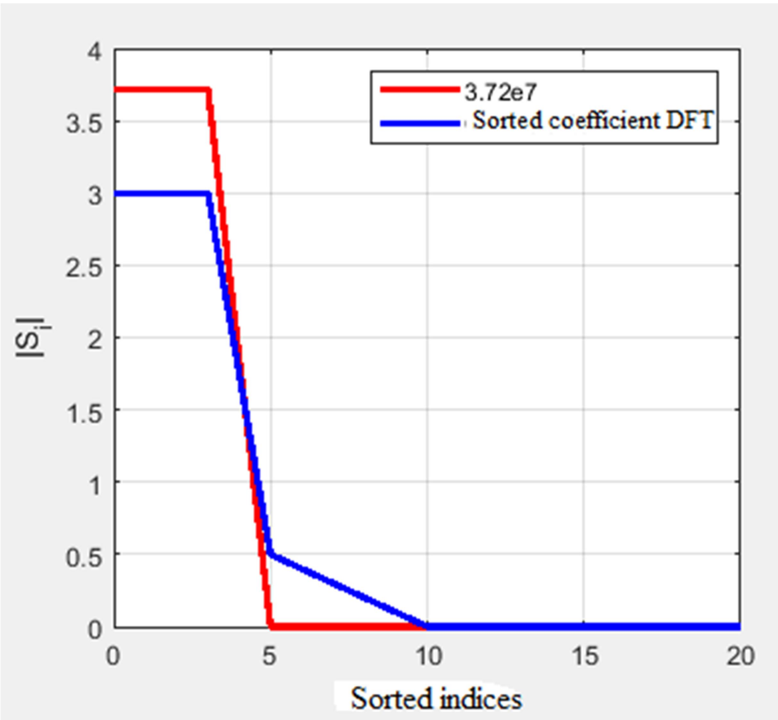

Fig. 13. *Compressibility of the Radar signal in the frequency domain and |Si |*

The test window is 1 second of data (80 million samples).

This result shows that the decrease in $(|S_i|)$ towards zero in the time domain as well as the time domain frequency is slow and relatively smaller than the decay in the frequency domain. Thus, the Radar signal is rather compressible in the frequency domain.

The module of the Fourier coefficients sorted in decreasing order follow a decrease in power law: $|S_i| = 3.72i^{-5}$ illustrated in figure 13 ;

with i the index of the coefficients sorted in the transformation base DFT^{-1}.

VIII. DIGITAL STUDY OF THE APPLICATION OF CS FOR THE RADAR SIGNAL

E. Simulation of the problem

A source S (a radar) emits a wave of given frequency f, which propagates in space and partially reflects on the targets C_1 and C_2 at a respective distance R_1 and R_2 , and equivalent radar surface SER_1 and SER_2 , illustrated by figure 14

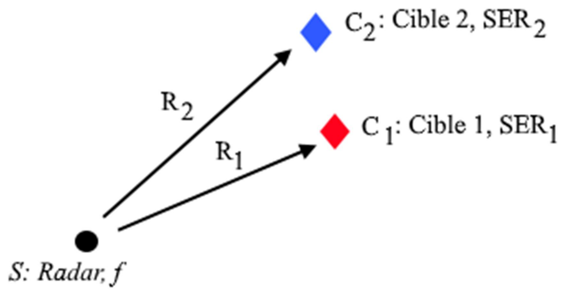

Fig. 14. *General schematic of the study*

To resolve the problem, we simulate this stage in two cases, namely:

- Very high frequency or VHF

Table 1 shows the parameters of our study for a very high frequency:

TABLE I. PARAMETER OF VHF

Number of cible n	2
Value of PRI	$100\mu s$
Frequency f	$50Mhz$
Position relative R	$50\ m$
Target position 1 R_1	$25\ m$
SER_1	$1\ m^2$
Target position 2 R_2	$35\ m$
SER_2	$2\ m^2$
Windowing	Hamming

The PRI is period Repetiton of Implusion.

In signal processing, windowing is used as soon as we are interested in a deliberately limited length. Indeed, a real signal can only have a limited duration in time. Moreover, a computation can only be done on a finite number of points. To observe a signal over a finite period of time, we multiply it by an observation window function.

Figure 16 illustrates the results obtained by parameter 1. The figure on the left illustrates the radar echo signal and on the right the result of the radar echo after simple compression.

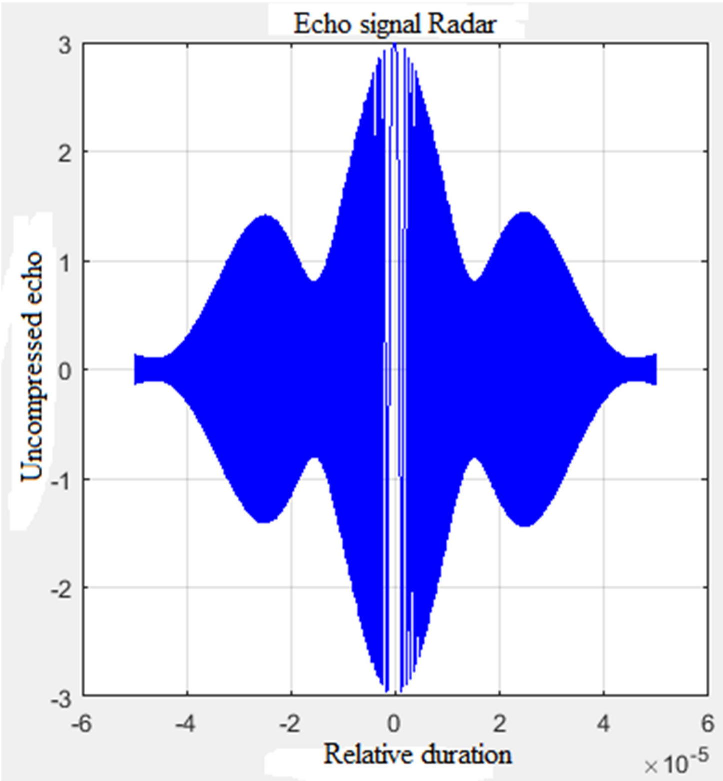

Fig. 15. *Echo signal (for VHF)*

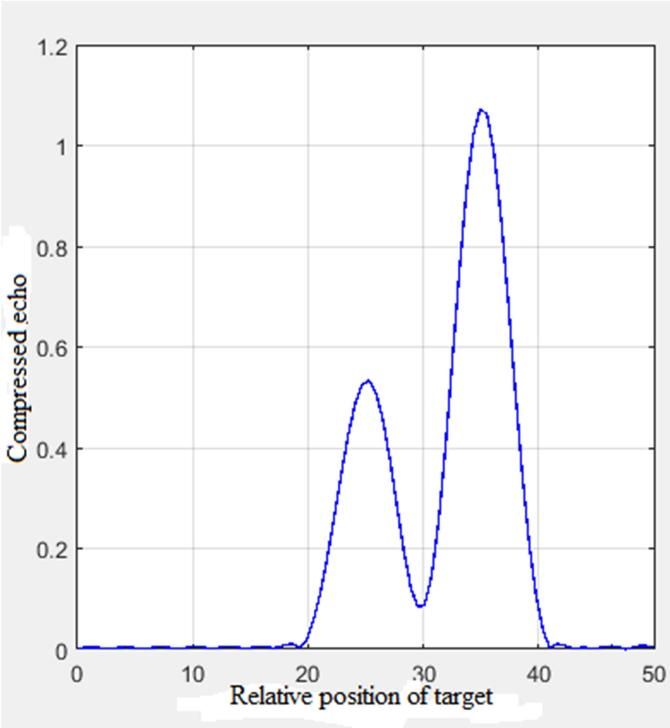

Fig. 16. *Echo signal after compression (for VHF)*

We note the presence of two targets C_1 and C_2

- High frequency or HF

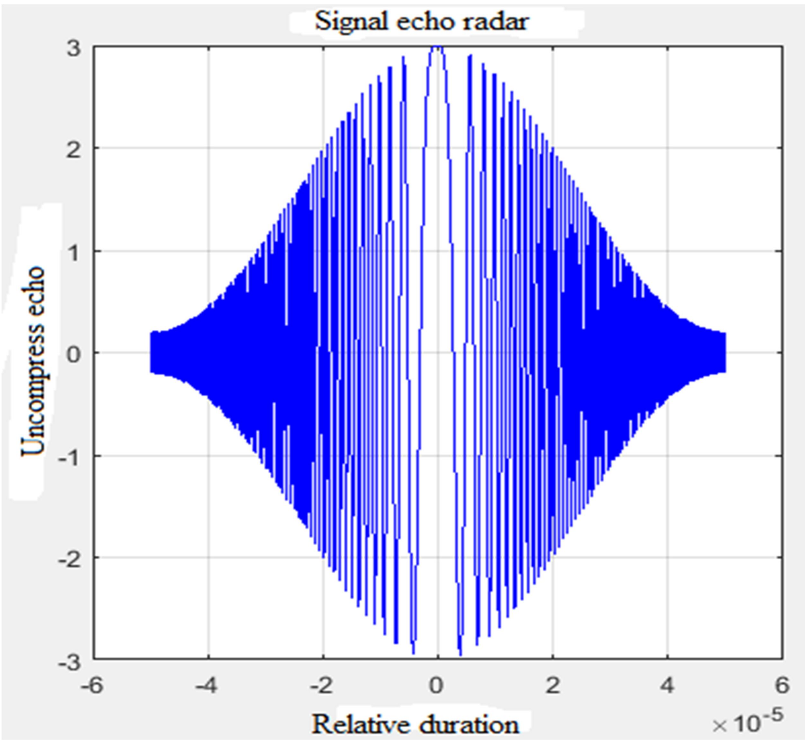

Fig. 17. *Echo signal (low frequency)*

Table 2 shows the parameters of our study for a high frequency:

TABLE II. PARAMETER FOR HF

Number of cible n	2
Value of PRI	$100\mu s$
Frequency f	$6Mhz$
Position relative R	$50\ m$
Target position 1 R_1	$25\ m$
SER_1	$1\ m^2$
Target position 2 R_2	$35\ m$
SER_2	$2\ m^2$
Windowing	Hamming

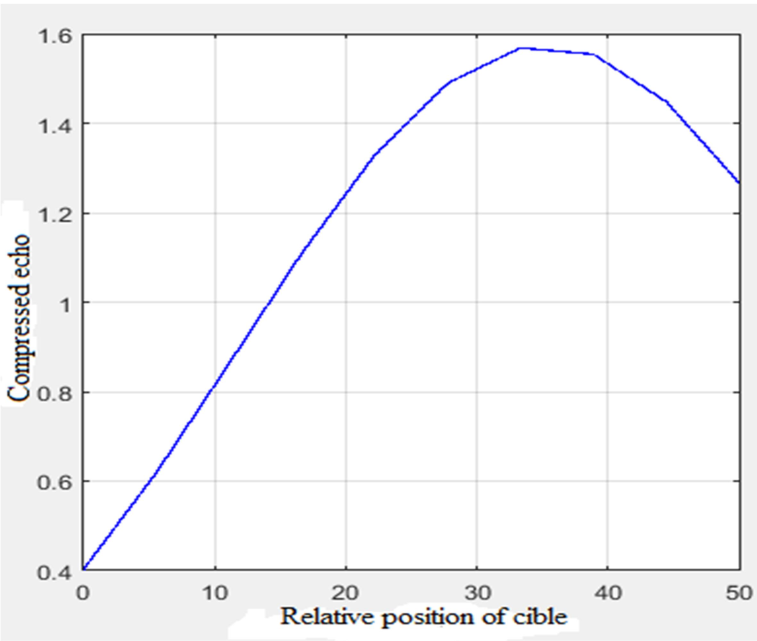

Fig. 18. *Echo signal after compression (for HF)*

Figure 18 illustrates the results obtained by parameter 2. The figure on the left illustrates the radar echo signal and on the right the result of the radar echo after simple compression. (Result after sampling based on Nyquist-Shanon condition and pulse compression by LFM)

Contrary to figure 16, we cannot distinguish the two targets C_1 and C_2 due to low frequency. In Figure 16 and Figure 18, we used Hamming windowing as an observation window function.

F. **Numerical simulation of the proposed solution**

In this paragraph, we apply the CS for the radar signals and we keep the same value in the previous parameter 2, whose frequency is low. (For N = 1028 and M = 171).

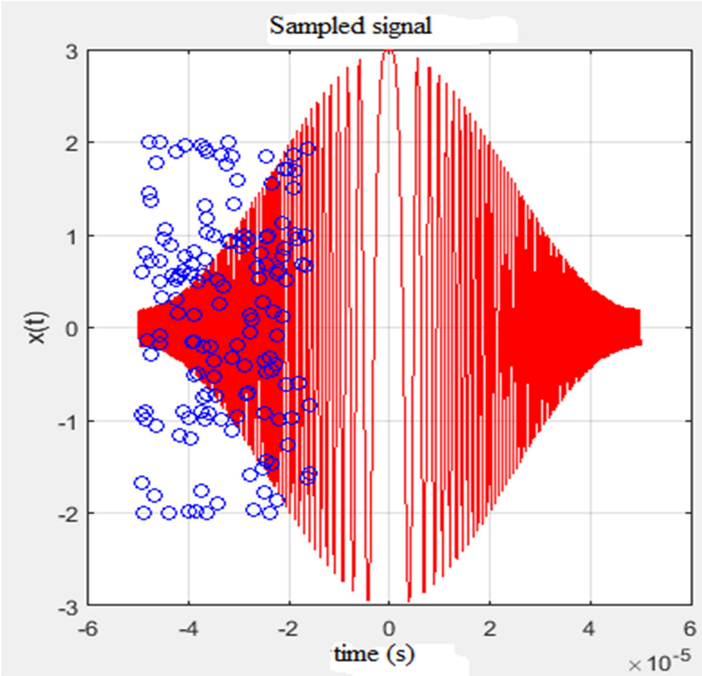

Fig. 19. *Sampled echo signal*

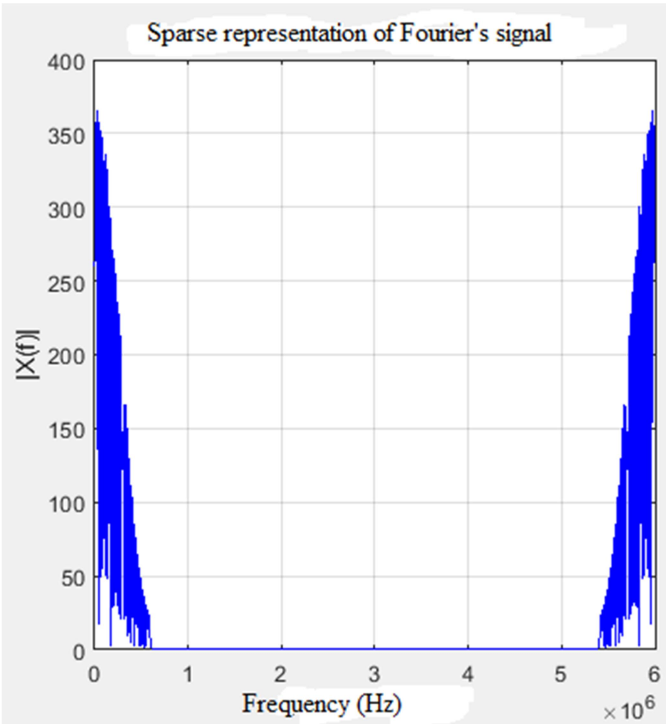

Fig. 20. *Sparse representation of the fourrier signal*

Sparse Fourier Transformation (SFT) is a technique used in NUS to compute outputs with a lower complexity than the method based on Fast Fourier Transformation (FFT). With SFT, data streams can be processed 10 to 100 times faster than with FFT, i.e. using FFT you have to process the whole sequence, then the non-zero values to get all the desired output.

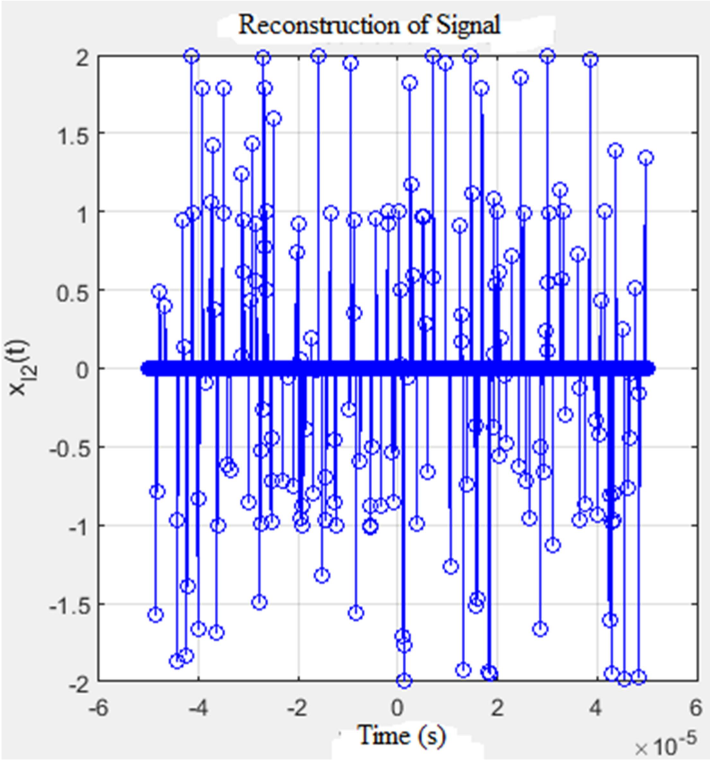

Fig. 21. *reconstruction of signal*

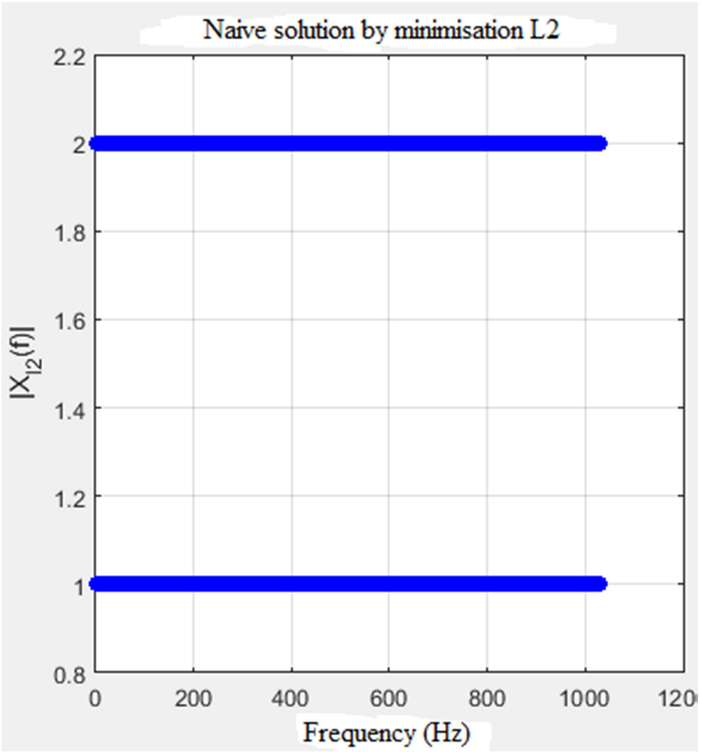

Fig. 22. *Minimization solution* L_2 *naïve*

To analyze a data set made up of P signals, there are different ways. These techniques are grouped under the name of Component Analysis, where components is synonymous with atom.

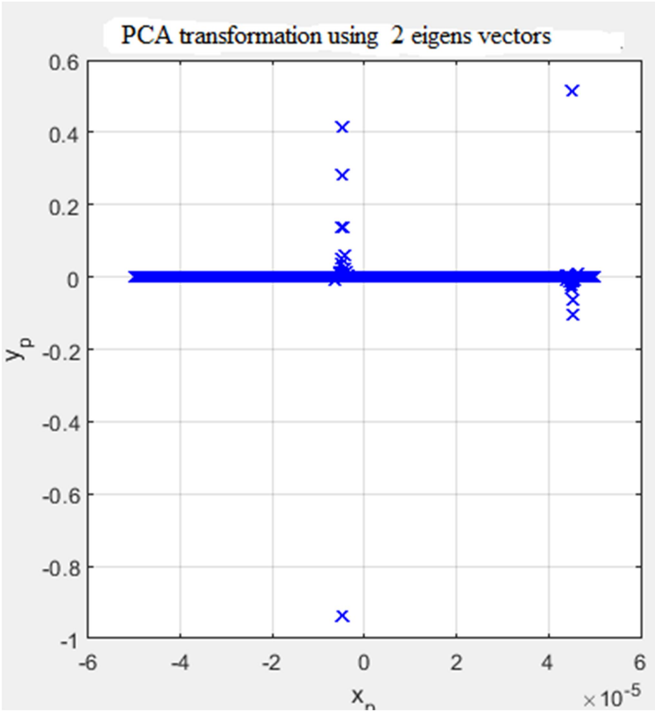

Fig. 23. *Transformation PCA with 2 eigen vectors*

Fig. 24. The Principal Component Analysis or PCA (Principal Component Analysis) is widely used to obtain an adapted base learned from the data, and to carry out dimension reduction.

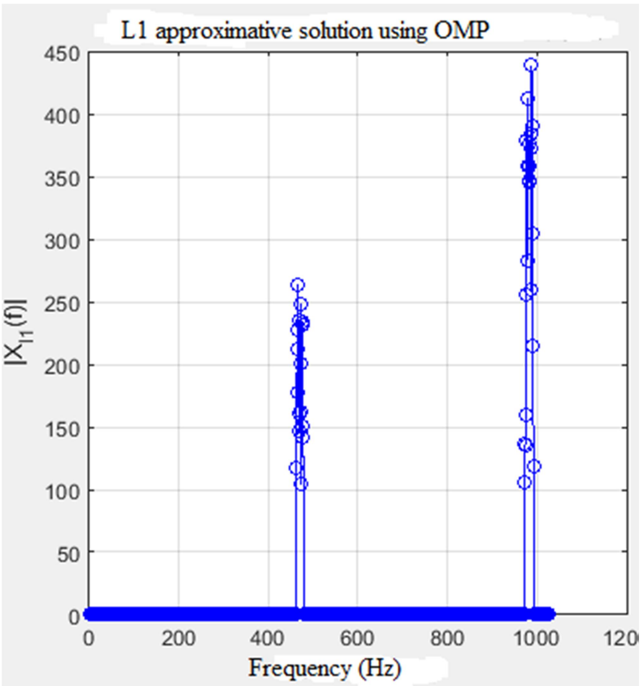

Fig. 25. Approximate solution of L_1 using OMP

Figures 19, 20, 21, 22, 23 and 24 respectively represent the sampled echo signal, sparse representation of the Fourier signal, signal reconstruction, minimization solution L_2 naïve, PCA transformation (Principal Component Analysis) with 2 eigenvectors and approximate solution of L_1 using the OMP reconstruction algorithm. These figures illustrate the stages of the NUS architecture.

By analyzing these results, figure 22 shows that the minimization solutions L_2 have the same as those of the values of SER_1 et SER_2 i.e $\left|X_{L_2}(f)\right| = \{1,2\}$. The approximate solution of L_1 , shown in figure 24 shows two sharp pulses corresponding to the numbers of targets (C_1 and C_2). Unlike the simple method in Figure 18, one can distinguish targets from these pulses. We can say that the technique of compressed acquisition (or compressive sensing) is more efficient in terms of reconstruction and precision in the sampling domain even if the frequency is low.

IX. Conclusion

Our study allowed us to know that it is not necessary to invest a lot of resources to observe the inputs of a sparse signal where most of these inputs are anyway zero. Using Compressive Sensing techniques, the signal is pre-encoded at the transmitter, which is being sent to the receiver through a wireless channel. This will increase the transmission data rate compared to current Radar communication systems. The design of Compressive sensing for the case of the Radar signal requires several steps: the choice of a basis of sparse appropriate to the studied signal, the determination of the level of compressibility, the selection of the measurement matrix as well as the architecture adapted to the signal. acquisition of the signal, and finally the choice of the reconstruction algorithm. The analysis of results, showed us that by applying the CS for the radar signal makes it possible to offer a better reconstruction and a better precision in terms of sampling and compression compared to those of Nyquist-Shannon and pulse compression. .

References

[1] N. Levanon, E. Mozen *« RADAR signal», John Wiley and Sons Inc»*, 2004

[2] N. Pandey, *« Beamforming in MIMO Radar »*, Department of Electronics and Communication Engineering National Institute of Technology Rourkela 2014

[3] Curry, G. R., *«Radar System Performance Modeling»,* Artech House, Norwood, 2001.

[4] M. Lustig, David L Donoho, J. M Santos et John M Pauly *«Compressed sensing mri ».* IEEE Signal Processing Magazine, 2008.

[5] M.A Davenport, Marco F Duarte, Yonina C Eldar et Gitta Kutyniok *« Introduction to compressed sensing. ».* Preprint, 2011.

[6] E. Candes, J. Romberg *«Sparsity and incoherence in compressive sampling».* Inverse problems,2007

[7] S.Qaisar, R. Muhammad Bilal *«Compressive sensing: From theory to applications»,* a survey. Journal of Communications and networks, 2013.

[8] S. G Mallat et Z. Zhang *«Matching pursuits with time-frequency dictionarie*s», IEEE Transactions on signal processing, 1993.

[9] Y. Chandra Pati, R.Rezaiifar *«Orthogonal matching pursuit: Recursive function approximation with applications to wavelet decomposition. In Signals, Systems and Computers»,* IEEE Transactions on signal processing, 1993.

[10] M. A Lexa, M. E Davies et J. S Thompson: *«Reconciling compressive sampling systems for spectrally sparse continuous-time signals. ».* IEEE Transactions on Signal Processing, 2012.

[11] M.Mishali et Yonina C Eldar : From theory to practice : *«Sub-nyquist sampling of sparse wideband analog signals. Selected Topics in Signal Processing».* IEEE Journal of, 2010.

[12] E. Candes *« Sparse Representations for Radar»* http://www.raeng.org.uk/publications/other/

[13] J. Wang, S. Kwon, P. Li et B. Shim *«Recovery of sparse signals via generalized orthogonal matching pursuit»* A new analysis. IEEE Transactions on Signal Processing, 2016

[14] S. Rapuano *«Analog-to-information converters research trends and open problems»*. In 2016 26th International Conference Radioelektronika, 2016.

[15] Ankit Kundu et Pradosh K Roy *«Sparse signal recovery from nonadaptive linear measurements»,* 2013.

[16] SparseLab. URL: https://sparselab.stanford.edu/